Chapter 1

# Are Ionic Liquids Suitable as New Components in Working Mixtures for Absorption Heat Transformers?

El-Shaimaa Abumandour, Fabrice Mutelet and Dominique Alonso

Additional information is available at the end of the chapter

http://dx.doi.org/10.5772/65756

**Abstract**

The working mixture almost exclusively used to operate absorption heat transformers (AHT) is {$H_2O$ + LiBr} ({$H_2O$ + $NH_3$} can also be used). Unfortunately, both working pairs present some drawbacks: corrosivity, toxicity, crystallization or high working pressure. Ionic liquids (ILs) possess very interesting properties (thermal stability, possible miscibility with water, negligible vapor pressure) that make them good candidates to be used as absorbents in AHT. This paper aims at providing an overview of available thermodynamic data concerning {$H_2O$ + IL} mixtures that could be used to operate an AHT.

**Keywords:** absorption heat pump, waste heat, ionic liquids, absorption heat transformers, thermodynamic properties, coefficient of performance

## 1. Introduction

Most of the industrial and domestic activities require large amounts of thermal energy to generate steam or heat by burning fossil fuel. After being used and degraded, low temperature heat is released to the environment as low grade waste heat. Large quantities of low temperature thermal waste heat streams from many industrial facilities such as power plants are discharged as thermal pollutants to the air and to the water at temperatures ranging from 60 to 100°C on a daily basis [1].

Among heat-driven devices are the absorption cycles. They can be divided into three classes: absorption heat pump (AHP), absorption chiller (AC), and absorption heat transformer (AHT). Absorption cycles become of great interest since electrical energy is replaced with low grade or waste heat allowing both primary energy savings and energetic efficiency improvements [2]. Consequently, absorption cycles enhance the atmospheric conditions by reducing the

emissions of greenhouse gases. Environmental impacts of absorption cycles can even be reduced by the adoption of environmental friendly working mixtures [3, 4].

One of the key points to the performance of an absorption cycle is the working fluid used. Nowadays, the most used binary systems in the absorption heat cycle are {water + lithium bromide ($H_2O$ + LiBr)} and {ammonia + water ($NH_3$ + $H_2O$)}. The aqueous solution of LiBr is the most successful working mixture in absorption cycles and widely spread all over the world [2, 3]. Nevertheless, LiBr aqueous solution has some main drawbacks as follows:

- Absorption heat pumps cannot operate at an evaporation temperature below 0°C because of the use of water as a refrigerant, which makes it unusable for subfreezing refrigeration or heating/domestic hot water (DHW) supplementation in cold regions. Crystallization of {$H_2O$ + LiBr} at high concentrations is a common problem. High vacuum conditions should be preserved in the system for suitable operation of the {$H_2O$ + LiBr} system; otherwise, the performance of the absorption cycle would be greatly reduced [5]. {$H_2O$ + LiBr} is corrosive to metals [2–6].
- {$NH_3$ + $H_2O$} requires high working pressure and ammonia is toxic.

Due to these disadvantages, which have not been solved properly, the absorption technology has known a very limited expansion [7, 8]. That is why heat pump and absorption chiller technologies suffer from lack of suitable working pairs. Hence, searching for new beneficial and reliable binary systems (to overcome these technical limitations) has become of great importance lately.

Limited numbers of critical reviews have been published in the literature on the subject of absorption technologies. In 2001, Srikhirin et al. [6] reviewed different configurations and types of absorption refrigeration cycles and working pairs. Performance development and enhancement of absorption cycles were evaluated. They concluded that double-stage absorption refrigeration cycle based on {$H_2O$ + LiBr} has the highest coefficient of performance (COP) if compared to other systems in the market. In addition, they stated that multistage absorption cycles have a promising future.

In 2012, Sun et al. [3] have shown that {$H_2O$ + LiBr} and {$NH_3$ + $H_2O$} mixtures can be improved by the use of additives. They also stated that working pairs dedicated to specific applications such as solar or geothermal energy should use hydrofluorocarbons (HFCs) as a refrigerant.

Ionic liquids (ILs) are environmentally friendly solvents, which have attracted considerable attention recently. Ionic liquids are salts in liquid state having melting point below some arbitrary temperature, such as 100 °C (373 K). These solvents consist of ions (an asymmetric, large organic cation, and organic or inorganic anion). A great advantage of ILs is that their physical properties such as melting points, density, and hydrophobicity can be adjusted to design different types of ILs that can be used for various applications.

It is now well established that ILs exhibit interesting physicochemical properties allowing their use for various industrial applications [1–10].

ILs could be used as alternative working mixtures in absorption heat pump cycles. Hence, the possibility to have ionic liquids with a low melting point (lower than the temperature of the

cold heat source of absorption heat pumps) allows overcoming the crystallization problem of the {water + LiBr} solution that can occur under some conditions [2]. Moreover, aqueous solution of ionic liquids seems to be less corrosive than the {water + LiBr} solutions. Finally, many ionic liquids show a high miscibility with water, which is a recommended refrigerant for absorption cycles (high latent heat, low viscosity, nontoxic, etc.). Consequently, the analysis of binary systems composed of {ILs + water} for this application has to be explored [10].

Few papers were published concerning working fluids containing ILs and a refrigerant such as $NH_3$, water, ethanol, or halogenated hydrocarbon series. Although many working fluids are proposed in the literature, there is not a complete review with comparison of their properties and performances. Studies mainly focus on the evaluation of {$H_2O$ + IL} systems for their potential use in absorption heat cycles [11, 12]. Khamooshi et al. [2] studied the performance of different working fluids containing ILs and different types of refrigerants in order to define the most suitable binary system. The coefficient of performance obtained on binary systems {$H_2O$ + ILs} in absorption cooling cycle is lower than {$H_2O$ + LiBr}. Nevertheless, the COP of these systems is higher than 0.7.

In 2014, Zheng et al. [13] presented a compilation of thermodynamic properties of binary systems containing {$H_2O$ or $NH_3$ or HFCs or alcohols + ILs}. The simulation of IL working fluids for single effect absorption cooling cycles showed that several binary systems have a real potential.

Publications concerning the development of working fluids and absorption cycles almost exclusively focus on air conditioning and refrigeration. It seems that no previous review has comprehensively summarized the studies and applications of absorption heat transformers using {$H_2O$ + ILs} as the working fluid. Recently, IoLiTec has developed working mixtures composed of {$H_2O$ or $NH_3$ + ILs} for absorption cycles and filled the first patent application in this field in 2004, which is now owned by BASF. Meanwhile, other companies, such as DuPont and Degussa, are interested in using ILs in absorption cycles. This ensures the great potential of ILs in this application. Encouraging the use of ILs in this technology in combination with upgrading industrial and other waste heat could enhance the conservation of fossil fuels and hence decrease the emissions of greenhouse gases [14].

This work mainly focuses on the study of binary systems {$H_2O$ + ILs} in absorption heat transformers. The first part of the paper briefly describes the absorption cycle. Then, the thermodynamic and physical properties of the binary systems {$H_2O$ + IL} are summarized and the influences of the IL structure on these properties are presented. In this section, results found in the literature about the performance of absorption cycles using {$H_2O$ + IL} as working mixtures are also presented. The last section of this paper is devoted to the calculation of the coefficient of performance of an AHT operated with each binary system {$H_2O$ + IL}.

## 2. Absorption heat cycles

Absorption cycles perform heat exchange between several heat sources or sinks. In the simplest case, there are three heat reservoirs characterized by their relative temperature level (high, medium, and low) as shown in **Figure 1**.

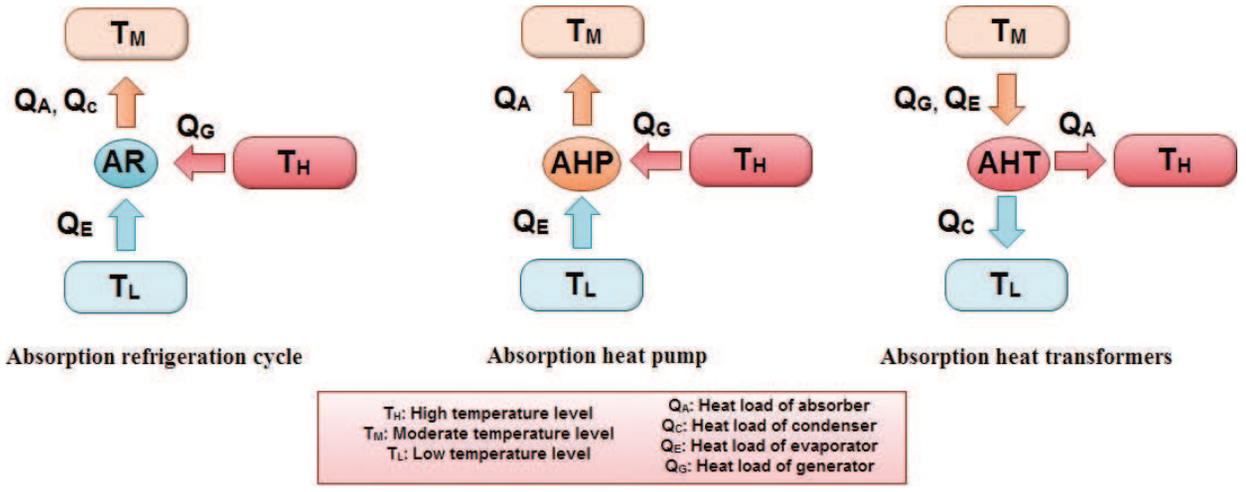


**Figure 1.** Simple absorption cycle.

Absorption systems can operate according to different modes differing by the nature of the driving heat and by the desired useful effect. These modes are as follows:

- Refrigerator: The driving heat is provided to the absorption cycle by a high temperature heat source. The low temperature source also provides heat to the cycle producing the cooling effect (useful effect). Heat is released to the medium temperature heat sink (generally the environment).
- Heat pump: As well as in a refrigerator, the cycle is driven by the heat provided by the high temperature source. The cycle also receives heat from the low temperature source. The useful heat is released to the medium temperature sink (generally a building or process that requires to be heated).
- Absorption heat transformer: Compared to both previous modes, sink and sources are reversed. The driving heat is a medium temperature heat (generally a waste heat). The upgraded useful heat is rejected to the high temperature sink and degraded heat is rejected to the low temperature sink (generally the environment).

Absorption cycles are composed of five main components: evaporator, condenser, generator, absorber, and solution heat exchanger (economizer) (**Figure 2**). They generally use a binary working mixture composed of a low boiling component called the refrigerant and a high boiling component called the absorbent.

In an absorption heat transformer (**Figure 3**), the driving heat (medium temperature waste heat) is provided to the mixture of an absorbent and a refrigerant (weak solution) in the generator at a low pressure producing two streams: a pure refrigerant vapor stream and a liquid mixture stream (strong solution).

This vapor is condensed in the condenser releasing heat to the low temperature heat sink. The condensate is increased to high pressure through a pump and vaporized in the evaporator, thanks to medium temperature heat. The strong solution passes through a pump to high pressure and is sent to the absorber where it absorbs the vapor produced in the evaporator.

http://dx.doi.org/10.5772/65756

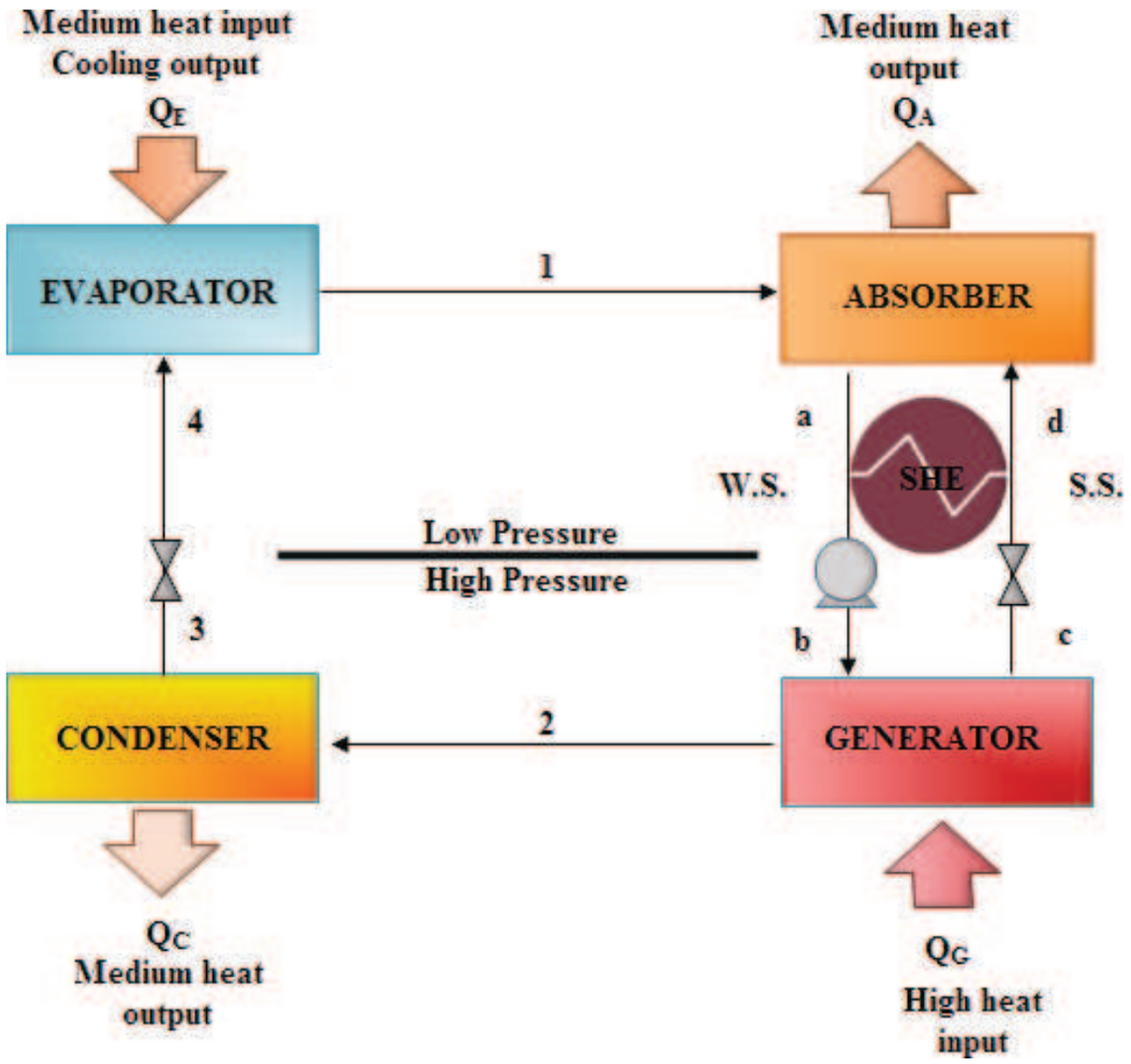


**Figure 2.** Schematic diagram of an absorption refrigeration cycle; A: absorber, C: condenser, E: evaporator, G: generator, SHE: heat exchanger.

This operation releases high temperature useful heat. The resulting weak solution is throttled through a valve and sent back to the generator. The solution heat exchanger allows preheating the strong solution entering the absorber by exchange with the weak solution leaving the absorber [15]. In refrigeration or heat pump absorption cycles (**Figure 2**), pressure levels are reversed (high pressure in the generator and in the condenser and low in the evaporator and the absorber), high temperature heat is provided to the generator, low temperature heat is provided to the evaporator and medium temperature heat is rejected at the condenser and absorber.

The working mixture properties will directly affect the absorption cycle performance. The following criteria can be followed to properly choose a working mixture [3]:

**i.** The presence of absorbent in the refrigerant must increase as high as possible the boiling point of the solution.

**ii.** In order to reduce refrigerant flow rate, its vaporization latent heat has to be as high as possible.

**i.** In order to reduce exchange areas, pressure decreases and more generally the size and cost of equipment, viscosity of the solutions have to be the lowest as possible whereas thermal conductivity and diffusion coefficient have to be the highest as possible.

**ii.** Components of the working mixture should not be too expensive.

**iii.** Components of the mixtures should be noncorrosive and nontoxic.

**iv.** The environmental impact of the working mixture should be the lowest as possible, especially in terms of GWP and ODP.

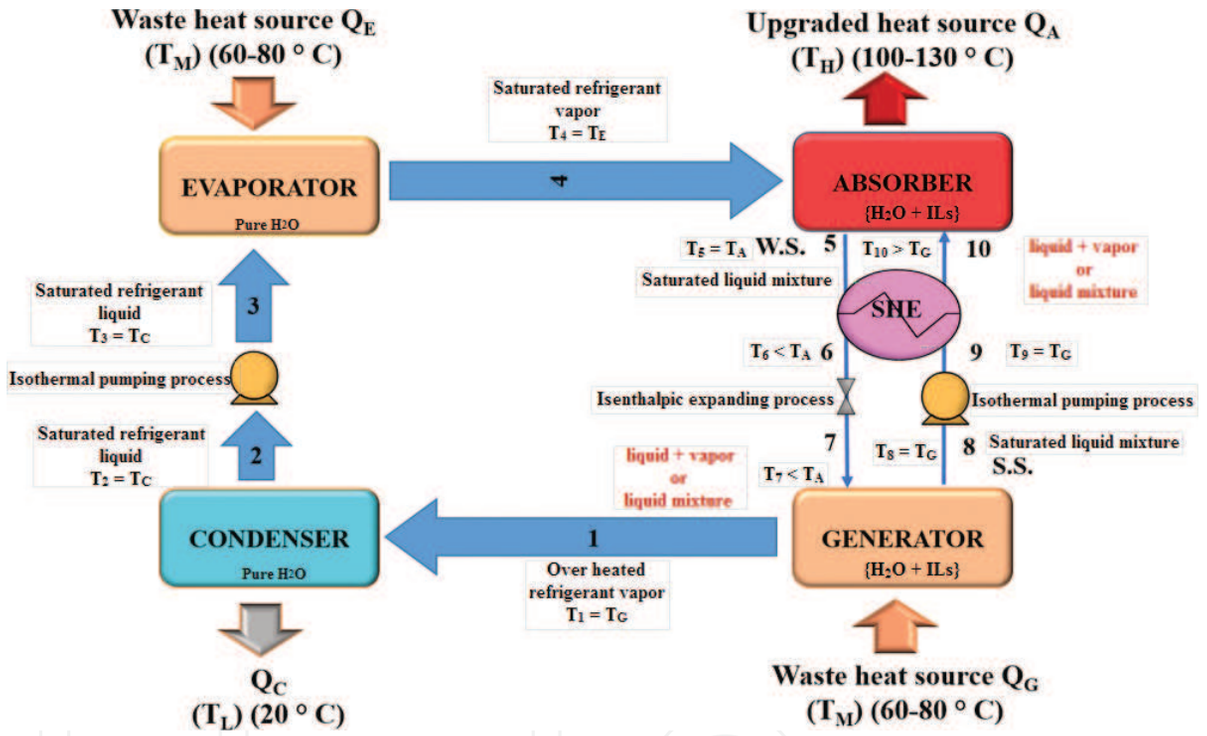


**Figure 3.** Schematic diagram of an absorption heat transformer; A: absorber, C: condenser, E: evaporator, G: generator, SHE: heat exchanger, P1 and P2: pump, v: valve.

To assess the energetic performance level of an absorption cycle, a criterion was defined: the coefficient of performance. Its expression depends on the kind of absorption cycle (refrigeration, heat pump, or AHT). Nevertheless, it is possible to define it as the ratio of the useful heat flow exchanged to the costly heat flow consumed [1]. For example, in a refrigeration cycle the expression of COP becomes [7–16]:

$$\mathrm{COP} = \frac{\text{Low temperature heat flow exchanged at the evaporator}}{\text{Hig htemperature heat flow provided at the generator} + \text{Mechanical pumping power}} \quad (1)$$

For an absorption heat transformer the COP expression is [8]

$$COP = \frac{\text{H. temp. heat flow exchanged at the absorber}}{\text{M. temp. heat flows exchanged at the generator and evaporator} + \text{Mechanical pumping power}} \quad (2)$$

## 3. Working fluids containing {water + ILs} for absorption cycles

Water can be considered as a green refrigerant, nontoxic, having high latent heat and excellent thermal characteristics. ILs used in the working fluids {$H_2O$ + ILs} have to be hygroscopic and stable in aqueous solution. Numerous articles have studied the behavior of ILs with water, but there is still a lack of thermodynamic data for such mixtures.

### 3.1. {$H_2O$ + ILs} binary systems in the literature

Recently, the performances of binary mixtures {$H_2O$ + IL} have been evaluated as alternative binary systems in the absorption cycle [16–18, 19]. Numerous articles present thermodynamic studies of binary systems containing water and IL. **Table 1** lists the most studied ILs in the literature and the thermophysical properties available. Alkylsulfate- and alkylphosphaste-based ILs are well known, and their performance in working fluids {$H_2O$ + IL} was evaluated in different absorption cycles [7–26].

The binary systems {$H_2O$ + dialkylimidazolium alkylphosphate}, 1-dimethylimidazolium dimethylphosphate, and 1-ethyl-3-methylimidazolium dimethylphosphate were extensively studied in numerous papers, where not only the data of vapor-liquid equilibria (VLE) but also density, viscosity, heat capacity, and excess enthalpy are available [7–25, 27–29]. These data make it possible to simulate the performance of these binary mixtures as working fluids in the absorption refrigeration cycle [7–25, 27, 30]. The simulation results show that the cycle performance of both systems is lower but close to the value obtained with the conventional working pair {$H_2O$ + LiBr}. Yokozeki and Shiflett [31] also examined the feasibility of different binary systems {$H_2O$ + IL} in an absorption cooling cycle and they found out that the best system is {$H_2O$ + [EMIM][DMP]}.

The performance of {$H_2O$ + LiBr} is still higher with a COP of 0.78 and a solution flow rate 53% smaller than [EMIM][DMP]. Nevertheless, the use of {$H_2O$ + [DMIM][DMP]} as the working fluid enables to work in a large range of temperatures and to stop crystallization and corrosion caused by {$H_2O$ + LiBr}. Several papers were focused on the measurements of thermodynamic properties of the binary system {$H_2O$ + [EMIM][$EtSO_4$]} [16–25, 27, 30, 32], {$H_2O$ + [EMIM][Ac]} [33, 34], or {$H_2O$ + [HOEtMIM][Cl]} [35]. Even if these systems have some interesting properties such as low density and heat capacity or strong negative deviations from Raoult's law, no simulation of the performance of these working fluids in an AHT was presented.

## 4. Thermodynamic properties of {$H_2O$ + IL}

The knowledge of thermodynamic properties, phase behavior, and safety/environmental hazards of {$H_2O$ + IL} is required for the evaluation of this system in an AHT. The following section presents the behavior of ILs in the presence of water and the influence of their structure on thermodynamic properties.

| ILs | Refrigerant | VLE measuring methods | Thermo. Para. | References |
|---|---|---|---|---|
| **1,3-dimethylimidazolium chloride [DMIM][Cl]** | Water | B. P. method | $\rho$ | [57] |
| **1,3-dimethylimidazolium dimethylphosphate [DMIM][DMP]** | Water | B. P. method | $Cp$, $\rho$, $H^E$, | [7, 24, 28–30] |
| **1-(2-hydroxyethyl)-3-methylimidazolium chloride [HOEtMIM][Cl]** | Water | B. P. method | VLE, $Cp$, $\rho$ | [35] |
| **1-(2-hydroxyethyl)-3-methylimidazolium trifluoroacetate [HOEtMIM][TFA]** | Water | Fischer Labodest apparatus (model) | VLE data, $H^E$ | [16] |
| **1-ethyl-3-methylimidazolium tetrafluoroborate [EMIM][$BF_4$]** | Water | Static method | $\rho$ | [63] |
| **1-ethyl-3-methylimidazolium dimethylphosphate [EMIM][DMP]** | Water | B. P. method | $Cp$, $\rho$, $H^E$, viscosity | [8, 22, 25–27, 30] |
| **1-ethyl-3-methylimidazolium bis-(trifluoromethylsulfonyl)imide [EMIM][$Tf_2N$] or [$(CF_3SO_2)_2N$]** | Water | Static method | VLE data | [28] |
| **1-ethyl-3-methylimidazolium acetate [EMIM][Ac]** | Water | Dynamic method | $Cp$, $\rho$, viscosity | [33, 34] |
| **1-ethyl-3-methylimidazolium ethyl sulfate [EMIM][$EtSO_4$]** | Water | B. P. method and static method and Fischer Labodest apparatus | $Cp$, $\rho$, $H^E$, viscosity | [26, 28, 29, 31–45, 47–55] |
| **1-ethyl-3-methylimidazolium diethyl phosphate [EMIM][DEP]** | Water | Circulation still | VLE data, $H^E$ | [16–37] |
| **1-ethyl-3-methylimidazolium trifluoromethanesulfonate [EMIM][TFO] [Triflate]** | Water | Static method and Fischer Labodest apparatus | $Cp$, $\rho$, $H^E$ | [56] |
| **1-ethyl-3-methylimidazolium trifluoroacetate [EMIM][TFA]** | Water | Fischer Labodest apparatus | $Cp$, $\rho$, $H^E$ | [51] |
| **1-ethyl-3-methylimidazolium methanesulfonate [EMIM][$MeSO_3$]** | Water | | $H^E$ | [16] |
| **1-butyl-3-methylimidazolium tetrafluoroborate [BMIM][$BF_4$]** | Water | B.P. method &Static method | $Cp$, $\rho$, $H^E$, viscosity | [57] |
| **1-butyl-3-methylimidazolium trifluoromethanesulfonate [BMIM][$CF_3SO_3$] [TFO][triflate]** | Water | Isobaric microebulliometer | $Cp$, $\rho$, $H^E$ | [39–45, 47–56] |
| **1-butyl-3-methylimidazolium methanesulfonate [BMIM][$C_1SO_3$]** | Water | Isobaric microebulliometer | VLE data | [39] |
| **1-butyl-3-methylimidazolium chloride [BMIM][Cl]** | Water | Labodest apparatus | VLE data | [34, 35, 37–39] |
| **1-butyl-3-methylimidazolium bromide [BMIM][Br]** | Water | B. P. method & Isobaric microebulliometer | VLE data | [39] |
| **1-butyl-3-methylimidazolium acetate [BMIM][Ac]** | Water | Isobaric microebulliometer, static method | VLE data | [34, 35, 37–39] |
| **1-butyl-3-methylimidazolium trifluoroacetate [BMIM][$CF_3CO_2$]** | Water | Isobaric microebulliometer | VLE data | [39] |

| ILs | Refrigerant | VLE measuring methods | Thermo. Para. | References |
|---|---|---|---|---|
| **1-butyl-3-methylimidazolium thiocyanate [BMIM][SCN]** | Water | Isobaric microebulliometer, static method | VLE data | [39] |
| **1-butyl-3-methylimidazolium tosylate [BMIM][TOS]** | Water | Isobaric microebulliometer | VLE data | [39] |
| **1-butyl-3-methylimidazolium methylsulfate [BMIM][$MeSO_4$]** | Water | Labodest app. | Cp, $\rho$, $H^E$ | [56] |
| **1-butyl-3-methylimidazolium dibutyl phosphate [BMIM][DBP]** | Water | Ebulliometric method | VLE data | [36] |
| **diethylmethylammonium methanesulfonate ([DEMA][OMs])** | Water | Dynamic method | VLE data | [27] |
| **1-hexyl-3-methylimidazolium tetrafluoroborate [HMIM][$BF_4$])** | Water | | $\rho$ | [63] |

**Table 1.** Thermodynamic parameters of different binary systems composed of {water + ILs}.

### 4.1. Thermodynamic models for the representation of a binary system {$H_2O$ + IL}

A large number of thermodynamic models have been used to represent the phase diagrams of binary systems {$H_2O$ + IL}. Some groups show that the NRTL model can be successfully used to represent thermodynamic properties of systems containing ILs [7–25, 27–29, 32–37]. Alevizou et al. [38] also used the UNIFAC model to describe the phase equilibria of solvent/ionic liquid systems. While the ionic liquids were based on an imidazolium cation and a hexafluorophosphate anion, water was considered to be the refrigerant. Two new main groups, the imidazolium and the hexafluorophosphate groups, were introduced in UNIFAC. SAFT-type equation of state was also used to represent mixtures containing ILs. This equation is a good tool to evaluate the density of pure ILs, solute activity coefficients but also VLE or LLE of binary or ternary mixtures {solute 1 + solute 2 + IL} [39, 40]. Cubic equations of state such as Peng-Robinson (PR) and Soave-Redlich-Kwong (SRK) were also used to represent quite accurate VLE, bubble point data or critical points of systems containing ionic liquids, gases, and/or liquids [31, 33–35, 37–45].

### 4.2. Experimental thermodynamic data of {$H_2O$ + IL}

*4.2.1. Vapor-liquid equilibrium (VLE)*

The experimental techniques used for VLE measurements are a boiling point technique [16–25, 30, 35, 37, 38, 46], static apparatus [32], and a quasi-static ebulliometer method [37]. The boiling point technique is the most appropriate to study mixtures containing ILs. Most of the articles related to VLE measurements concerning the binary systems {$H_2O$ + IL} are listed in **Table 1**.

Activity coefficient can be calculated from VLE data. This parameter illustrating the deviation from ideality of the mixture can be used to investigate the interaction between $H_2O$ and ILs and the hydrophilicity of the IL [16–39]. Preferentially, ILs used in AHT might be hydrophilic

and completely water soluble. Therefore, good working pairs are those presenting a highly negative deviation from Raoult's law [47].

Most binary systems {water + ILs} present activity coefficients lower than unity. The deviation from Raoult's law of {$H_2O$ + IL} is proportional to the IL content [17–19, 23–33, 36]. With respect to the anion, Ficke [16] has shown that the $\gamma$ values decrease according to: $[(CF_3SO_2)_2N]^- > [BF_4]^- > [EtSO_4]^- > [lactate]^- > [CH_3SO_4]^- > [glycolate]^- > [(CH_3)_2PO_4]^-$.

It is important to note that dialkylimidazolium $[(CF_3SO_2)_2N]$ with water present a miscibility gap [28]. The ability of IL to increase the water boiling temperature can be estimated using a simple relationship based on solvation model's parameters such the hydrogen-bond basicity [48].

Studies on water sorption by imidazolium-based ILs with anions $[Cl]^-$, $[BF_4]^-$, $[Br]^-$, $[Tf_2N]^-$, and $[PF_6]^-$ show that ILs with the shorter alkyl chain length lead to the highest water sorption capacity [7, 25–37]. Moreover, it was found that imidazolium cation is more efficient than pyridinium cation [49]. Cao et al. [49] also studied the anion effect on water sorption for nine ILs with $[BMIM]^+$ cation and they found that ILs followed this trend $[Ac]^- > [Cl]^- > [Br]^- > [TFA]^- > [NO_3]^- > [TFO]^- > [BF_4]^- > [Tf_2N]^- > [CHO]^- > [PF_6]^-$. The nature of the IL anion plays an important role on the boiling temperatures and its impact is as follows: $[CF_3SO_3]^- < [SCN]^- < [CF_3CO_2]^- < [TOS]^- < [Br]^- < [C_1SO_3]^- < [C_1CO_2]^-$ [39]. This work shows clearly that the observed trend is related to the anion and to its capacity to interact with water. Other research groups confirmed that anion has an essential rule that aiming to lower the vapor pressure of water $H_2O$ [25, 27, 30, 32, 33]. Seiler et al. [50] have shown that some ILs such as acetate and chloride-based ionic liquids are not suitable for absorptions cycles due to their insufficient stability and/or too high corrosion rates.

All VLE of binary systems {$H_2O$ + IL} found in the literature have been correlated using the NRTL model. The average relative deviations on activity coefficient and pressure obtained using the NRTL model range between 0.01 and 3.5%. Deviations of the 35 investigated systems are within ±13%.

### *4.2.2. Heat capacity*

Heat capacity evaluates the heat storage capacity of a fluid [51]. Only one theoretical model based on an artificial neural network is proposed in the literature to predict the heat capacity of binary systems containing ILs [52]. This approach gives good estimate of $C_p$ of mixtures containing ILs with an average absolute relative deviation of about 1.60%.

In general, heat capacity is expressed using a temperature- and composition-dependent polynomial equation [35]:

$$C_p = \sum_{i=0}^{3} (A_{i+} B_i T) x m_2{}^i \tag{3}$$

where $C_p$ is the mass heat capacity in kJ $kg^{-1}$ $K^{-1}$, $A_i$ and $B_i$ are adjustable parameters, $T$ is the absolute temperature in K, and $xm_2$ is the mass fraction of ILs. We have correlated all heat capacity

data of {$H_2O$ + ILs} published in the literature using Eq. (3). The mass excess heat capacity, $C_p{}^E$ can be calculated from the heat capacities of the mixture and that of the pure compounds:

$$C_p^E = C_p - \sum xmi \cdot C_{P,i} \tag{4}$$

where $C_p$ is the mass heat capacity in kJ $kg^{-1}$ $K^{-1}$ of the mixture, $C_{p,i}$ is the mass heat capacity of the pure compound and *xmi* is its mass fraction.

The low mass heat capacity values of the binary systems {$H_2O$ + ILs} lead to reduce power consumption, beneficial to heat transfer and improves the COP in the absorption cycle [7, 26, 28, 29, 31, 33–45, 47–55].

*4.2.3. Excess enthalpy ($H^E$)*

$H^E$ is a key parameter for the simulation of the performance of AHT and it also gives an insight into the interactions between the molecules. Few $H^E$ data for binary systems {$H_2O$ + ILs} can be found in the literature. This leads to make the hypothesis that $H^E$ is equaled to zero in simulation.

Garcia-Miaja et al. [56] measured $H^E$ for different binary mixtures containing triflate or alkylsulfate or [BMPyr]-based ILs. All collected data show that the sign of $H^E$ is mainly related to the nature of the anion [56].

Kurnia and Coutinho [10] reviewed the behavior of $H^E$ for binary systems composed of {$H_2O$ + ILs}. They found that the conductor-like screening model for real system (COSMO-RS) is a successful estimating method to predict the behavior of the interaction between water and ILs. It is obvious from the literature [10–16] that the positive (endothermic) $H^E$ of the binary system mainly depends on the hydrogen bonding, water molecules, and hydrophobicity. Weak interaction between the water-IL binary system causes water to use the energy of the system to rearrange their molecules and the process turn to be endothermic and the reverse occurs in the case of the exothermic process. Ficke [16] stated that with the increase of the alkyl chain length the hydrophobicity increases hence decreasing the negativity of $H^E$.

$H^E$ data found in the literature are regressed using Redlich-Kister polynomials [25]:

$$H^E = xm_1 xm_2 \sum_{i=1}^{n} A_i xm_2^i \tag{5}$$

where $H^E$ is the excess enthalpy in kJ $kg^{-1}$, $A_i$ is the adjustable parameter, and $x\ m_i$ is the mass fraction of species $i$ ($i$ = 1, 2).

We used Eq. (5) to regress all $H^E$ data found in the literature.

*4.2.4. Density*

Density is an important property because its knowledge is necessary to evaluate the pumping cost in a process. The density of pure ILs roughly ranges between 1.1 and 1.6 g $cm^{-3}$. The density of an IL depends on the type of anion and cation, but the key parameter is the anion. Hydrophobicity of ILs has also an important effect on the density of binary mixtures {$H_2O$ + IL}. The hydrophobicity of a dialkylimidazolium-based IL increases with an increase of the

alkyl chain length [26, 31, 33–35, 37–45, 47–57]. Consequently, the density of such ILs decreases with the increase of the alkyl chain length.

An increase in water content or temperature causes a decrease in the density in most of the binary systems studied. Hence, physical properties of ILs can be adjusted to fulfill the needs of applications for hydrophilic ILs by adding water or changing the temperature [57].

The density data for the 19 investigated binary systems were fitted [35] using Eq. (6).

$$\rho = \sum_{i=0}^{3} (a_i + b_i T) {x_2}^i \tag{6}$$

where $\rho$ is the density of the solution in g cm$^{-3}$, $T$ is the absolute temperature in K, ${x_2}^i$ is the molar fraction of the ILs, and $a_i$ and $b_i$ are adjustable parameters.

Excess molar volume ($V^E$) is an important parameter for the process design while it gives information on the nonideality of the working fluid. In the case of binary mixtures {$H_2O$ + IL}, the sign of excess molar volumes is related to the structure of the IL (anion, cation, and alkyl chain length) [26, 31, 33–35, 37–45, 47–56, 58, 59]. Generally, the anion imposes the sign of $V^E$. Hydrophobic anions ([$BF_4$], [SCN], and [$CF_3SO_4$]) leading to repulsive interactions with water have positive excess molar volumes. Strong IL-$H_2O$ interactions observed with anions containing oxygen atoms lead to negative $V^E$ [26, 46, 60]. Gonzalez et al. [61] stated that $V^E$ behavior for their investigated binary systems according to the cation type has the following trend: imidazolium $V^E$ > pyridinium $V^E$ ≅ pyrrolidinium $V^E$. A full description of excess molar volumes of binary mixtures containing {$H_2O$ + IL} can be found in the recent review of Bahadur et al. [62].

#### *4.2.5. Viscosity*

It is well known that pure ILs have higher viscosity than other solvents such as water, methanol, and ethanol [26]. This may enlarge the AHT size (exchange area) and increase the power required for the pumping process [63]. Nevertheless, various publications [26, 31, 33–35, 37–67] stated that viscosity of ILs sharply decreases when temperature increases and/or ILs are mixed with water. Taking into account that AHT has a high generator and absorber temperature (between 80 and 150°C), the viscosity of the {$H_2O$ + ILs} should not be a limitation for their use as absorbents in AHT [36]. The viscosity of {$H_2O$ + ILs} binary systems decreases because of the weak interaction between the IL anion and cation so the mobility of ions increases and the viscosity decreases [67]. It was noticed that fluorinated anions have lower viscosity than other anions such as alkylsulfates [64].

#### *4.2.6. Thermal decomposition*

Thermal decomposition could possibly be one of the most important properties to measure during the initial screening of an IL, especially for the operating temperatures of the processes related to this work. Most of the decomposition temperatures of ILs are measured using weight loss thermogravimetric (TGA) experiments and selected data are given in **Table 2**.

Nevertheless, it must be kept in mind that data taken from TGA will not serve to determine the maximum temperature limit for working without decomposition of the IL because this technique overestimates the decomposition temperature [68–70]. The experimental procedure proposed by Seiler et al. [50] based on a long-time thermal decomposition analysis seems to be more appropriate.

The decomposition temperatures of ionic liquids containing the [$TF_2N$] anion are higher than others [16–45, 47–50, 53, 54]. Ficke [16] and Seiler et al. [50] have shown that the decomposition temperature of [EMIM]$^+$-based ILs ranges between 178°C and 388°C (**Table 2**). The decomposition temperature mainly depends on two structural parameters: the nature of the anion and the alkyl chain length [46, 50–52, 55–71]. Ficke et al. [55] found that [EMIM][$EtSO_4$] reacts with water to give [EMIM][$HSO_4$] and ethanol. Another negative effect of using ILs is their hydrolysis [72]. Kinetic of hydrolysis is governed by the pH and the temperature of system [73, 74]. [TOS]-, [DMP]-, [$BF_4$]-, and [$PF_6$]-based ILs are known to be unstable in the presence of water under specific conditions [75].

| IL | Decomposition temperature (°C) | References |
|---|---|---|
| [EMIM][TFA] | 178 | [16] |
| [EMIM][$EtSO_4$] | 355 | [16] |
| [EMIM][$HSO_4$] | 359 | [16] |
| [EMIM][$MeSO_4$] | 362 | [16] |
| [EMIM][TFO] | 388 | [16] |
| [EMIM][$MeSO_3$] | 335 | [16] |
| [EMIM][SCN] | 281 | [16] |
| [EMIM][DEP] | 273 | [16] |
| [EMIM][$PF_6$] | 375–348.29 | [15] |
| [EMIM][$BF_4$] | 412–393 | [4] |
| [OHEMIM][TFA] | 187 | [16] |
| [$P_{2444}$][DEP] | 314 | [16] |

**Table 2.** Decomposition temperature for miscible ILs.

## 5. Coefficient of performance (COP)

### 5.1. Simulation of the AHT cycle performance

This work focuses on single effect absorption heat transformers (AHT). The simulations used to evaluate the performance of the AHT were performed with the following assumptions [7–9, 16–76]:

**i.** Steady-state operation;

**ii.** Negligible heat loss;

**iii.** Pressure drops not taken into account;

**iv.** Outlets of the generator and the absorber are liquids at their bubble point;

**v.** Liquid and vapor at the outlet of the condenser and the evaporator are saturated;

**vi.** Enthalpy of the fluid is conserved through the throttling valve;

**vii.** Minimum temperature difference between strong and weak solutions equal 5°C in the heat exchanger;

**viii.** Pumping mechanical power is neglected compared to heat flow exchanged.

The steady-state simulation of such a process is achieved by solving mass and energy balance equations.

The generator can be described by the overall and ionic liquid mass balance and heat balance equations:

$$\dot{m}_7 - \dot{m}_1 - \dot{m}_8 = 0 \tag{7}$$

$$\dot{m}_7 x_7^m = \dot{m}_8 x_8^m \tag{8}$$

$$Q_G + \dot{m}_7 h_7 - \dot{m}_8 h_8 - \dot{m}_1 h_1 = 0 \tag{9}$$

The strong solution at the outlet of the generator is a saturated liquid,

$$p_8 = p(T_8, x_8^m) \tag{10}$$

where $T_8 = T_1 = T_G$ and $p_8 = P_1 = p_G = p_c$

The condenser can be described by

$$\dot{m}_1 = \dot{m}_2 = \dot{m}_3 = 1\text{kg.s}^{-1} \tag{11}$$

$$\dot{m}_1 h_1 - \dot{m}_2 h_2 - Q_c = 0 \tag{12}$$

For state point 2 (saturated liquid water at the condenser outlet), we have:

$$p_2 = p_c = p^s(T_c) \tag{13}$$

In the case of the evaporator:

$$\dot{m}_3 = \dot{m}_4 \tag{14}$$

$$\dot{m}_4 h_4 - \dot{m}_3 h_3 - Q_E = 0 \tag{15}$$

Vapor is saturated at the outlet of the evaporator, so for point 4, we have:

$$p_4 = p_E = p^s(T_E) \tag{16}$$

Balance equations for the absorber give:

$$\dot{m}_4 + \dot{m}_{10} - \dot{m}_5 = 0 \tag{17}$$

$$\dot{m}_5 x_5^m = \dot{m}_{10} x_{10}^m \tag{18}$$

$$\dot{m}_4 h_4 + \dot{m}_{10} h_{10} - \dot{m}_5 h_5 - Q_A = 0 \tag{19}$$

State point 5 is described by Eq. (20)

$$p_5 = p(T_5, x_5^m) \tag{20}$$

where $T_5 = T_A$ and $p_5 = p_A = p_E$

Then, the heat exchanger is characterized by the minimal temperature approach between hot and cold streams:

$$T_5(\text{hotinlet}) - T_{10}(\text{hotoutlet}) = 5\text{K} \tag{21}$$

Heat balance on the solution heat exchanger can be written:

$$\dot{m}_5 h_5 + \dot{m}_9 h_9 - \dot{m}_6 h_6 - \dot{m}_{10} h_{10} = 0 \tag{22}$$

where $\dot{m}_i$, $h_i$, $x_i^m$ ($i$ =1, 2, 3, …, 10) are, respectively, the mass flow rate (kg $s^{-1}$), specific enthalpy (kJ $kg^{-1}$), and the mass fraction of an absorbent (IL) of each stream. $p^s(T)$ is the saturated vapor pressure of $H_2O$ at temperature $T$ and $p(T, x)$ is the saturation pressure of the {$H_2O$ + ILs} solution at temperature $T$ with an ionic mole fraction $x$. They are obtained by the following relations [25]:

$$p(T, x) = x_2 \gamma_2 p_1^s(T) \tag{23}$$

$$p^s(T) = \exp\left(73.649 - 7258.2/T - 7.3037 * \ln(T) + 4.1653 * 10 - 6 * (T2)\right)/1000 \tag{24}$$

with $p$ is the total pressure, $x_2, \gamma_2$ and $p_1^s$ is the IL mole fraction in the liquid phase, ionic liquid activity coefficient for the liquid phase, and saturated vapor pressure of the refrigerant, respectively.

Usually, when simulating an absorption heat transformer, the temperature level of the waste heat source is known (the medium-temperature level) as well as the temperature of the environment that is used as cold heat sink (the low-temperature level). The objective temperature level of the upgraded heat is also an input in this problem (the high-temperature level). Hence, temperatures $T_G$, $T_E$, $T_C$ and $T_A$ of the generator, the evaporator, the condenser, and the absorber, respectively, are known and taken as independent variables in the present research.

The enthalpy of a liquid mixture is expressed as follows:

$$h = x_1^m h_1 + x_2^m h_2 + \Delta_{mix} h \tag{25}$$

with

$$h_1 = h_{ref} + \frac{1}{\rho_{1,liq,T_{ref}}} * (p - p_{ref}) + \int_{T_{ref}}^{T} C_{p,1} dT \tag{26}$$

$$h_2 = h_{ref} + \frac{1}{\rho_{2,liq,T_{ref}}} * (p - p_{ref}) + \int_{T_{ref}}^{T} C_{p,2} dT \tag{27}$$

where $h_1$ and $h_2$ are the enthalpy of pure liquid $H_2O$ and IL, $x_1^m$ and $x_2^m$ are the mass fraction of $H_2O$ and IL, respectively, $\Delta_{mix}h$ is mixing enthalpy of the system, which can be sometimes neglected. $C_{p,1}$ and $C_{p,2}$ are the heat capacity of $H_2O$ and IL, respectively. The reference state for enthalpy calculations is defined $T_{\text{ref}}$, $h_{\text{ref}}$, and $p_{\text{ref}}$, respectively, its temperature, enthalpy, and pressure. These parameters are chosen arbitrarily as being:

$h_{\text{ref}} = 0$

$T_{\text{ref}} = 273.15$ K

$p_{\text{ref}} = 101.325$ kPa

$\rho_{1,\text{liq,Tref}}$ and $\rho_{2,\text{liq,Tref}}$ are the densities of pure liquid water and pure IL at reference temperature and pressure, respectively.

The performance of the AHT is evaluated through different criteria. The main one is the coefficient of performance. Its expression is given in Eq. (2) as the ratio of useful heat flow produced at the absorber to the waste heat flows provided to the generator and to the evaporator (pumping work is neglected).

Among other meaningful criteria, $\Delta x^m$ is the difference between ionic liquid mass fractions in the strong and weak solutions.

$$\Delta x^m = x_8^m - x_5^m = x_s^m - x_w^m \tag{28}$$

If COP is used to represent the quantitative aspect of heat upgrading, the gross temperature lift $\Delta t$, which is the temperature level difference between the upgraded heat and the waste heat, provides a qualitative performance criterion. It is defined as follows:

$$\Delta t = T_A - T_E \tag{29}$$

Another important criterion is the solution circulation ratio $f$, which is defined as the ratio of the strong solution mass flow rate to the vapor mass flow rate:

$$f = \frac{\dot{m}_7}{\dot{m}_1 = \frac{x_s^m}{(x_s^m - x_w^m)}} \tag{30}$$

This criterion allows knowing if the use of one working mixture leads or not to high solution flow rate which is linked to the capital cost (cost of the required working mixture and pumps) and operating costs (pumping energy cost). Observed values of $f$ for the {$H_2O$ + LiBr} and {$H_2O$ + $NH_3$} systems are generally low (typically around 10 [2–16]).

Another criterion to assess system compactness is the available heat output per unit mass of refrigerant, $q$ (kJ kg$^{-1}$):

$$q = \frac{Q_A}{\dot{m}_1} \tag{31}$$

### 5.2. COP for the absorption refrigeration cycle

The performance of {$H_2O$ + ILs} as working fluids was mainly evaluated for the absorption refrigeration cycle. Zhang and Hu [27] estimated the COP of an absorption chiller using {water + [EMIM][DMP]} and {$H_2O$ + LiBr} mixtures under the same operating conditions. {$H_2O$ + [EMIM][DMP]} leads to a value of COP higher than 0.7 that is lower than that obtained with {$H_2O$ + LiBr}.

Under precise conditions, Kim et al. [63] found that the COP value for a {$H_2O$ + [EMIM][$BF_4$]}-based refrigeration cycle can reach 0.91, this good performance is linked to the suitable compatibility of water with [EMIM][$BF_4$] and to the excellent intrinsic properties of water as a refrigerant.

The {$H_2O$ + [DMIM][DMP]} mixture has been studied by Dong et al. [7] and was compared to {$H_2O$ + LiBr} in a single-effect absorption refrigeration configuration. The ionic liquid-based working mixture leads to close performance to those obtained with the conventional mixture. Nevertheless, {$H_2O$ + [DMIM][DMP]} presents the advantage to allow a wider temperature working range as well as avoiding corrosion and crystallization problems.

### 5.3. Absorption heat transformer

A VBA dedicated calculation code has been developed to evaluate the performance of {$H_2O$ + IL} mixture as a working fluid in an absorption heat transformer (**Figures 4** and **5**).

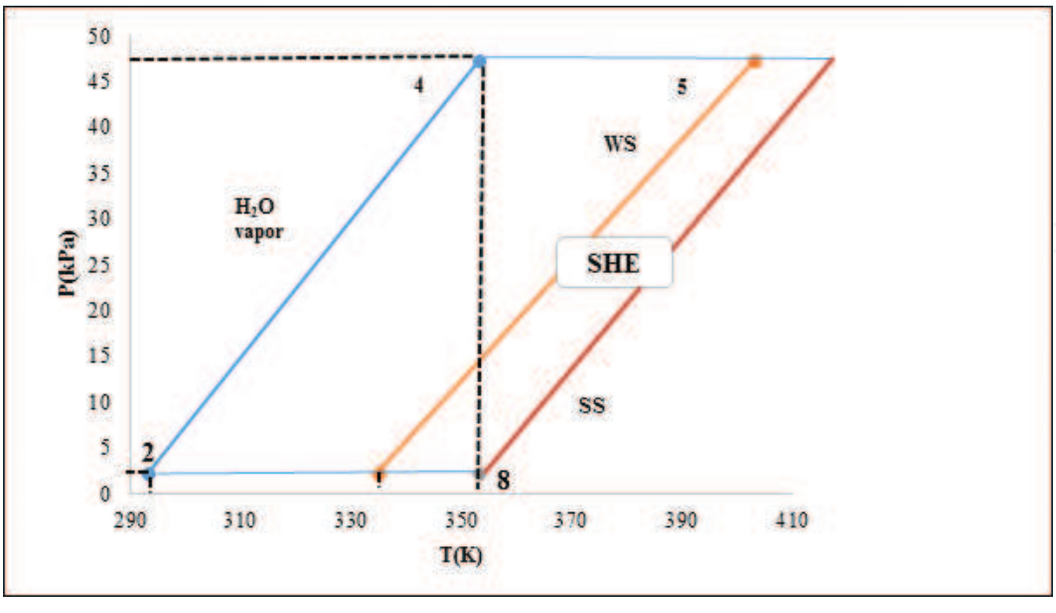


**Figure 4.** Thermodynamic cycle in absorption heat transformer (AHT).

Simulation results for both {$H_2O$ + IL} mixtures and conventional fluids as working fluids in AHT are presented in **Table 3**.

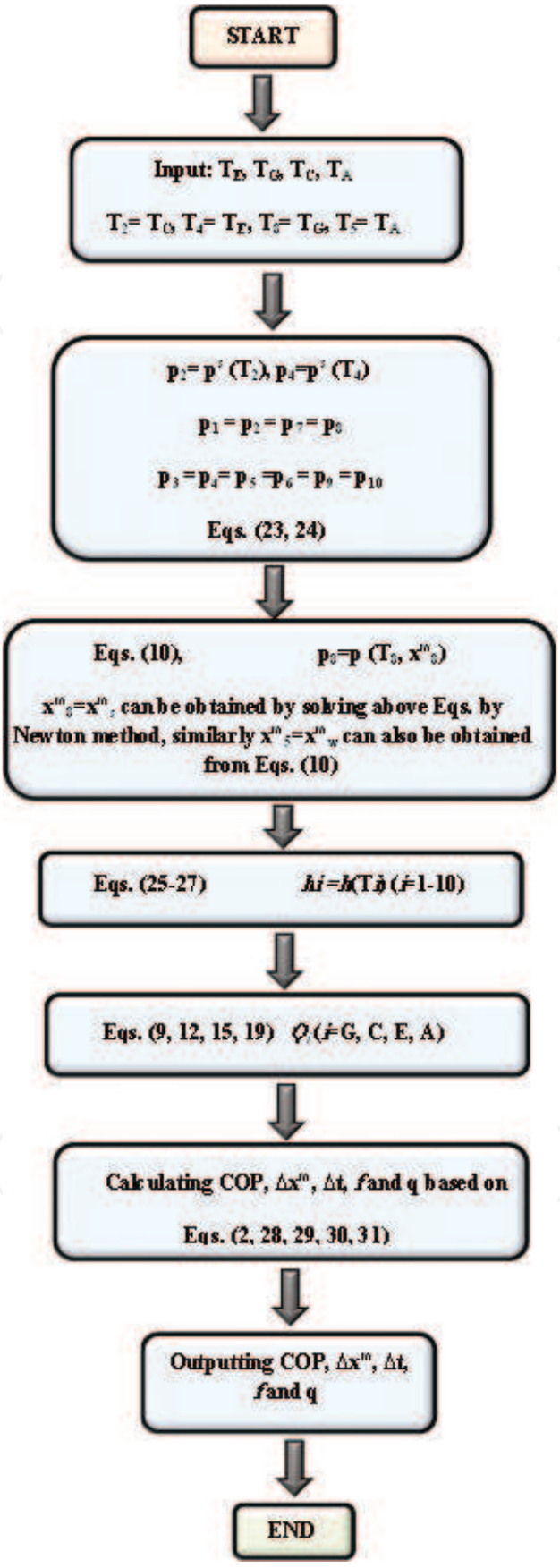


**Figure 5.** Flowchart for COP simulation.

| Refrigerant | Absorbent | COP | $x^m_s$ | $\Delta x^m$ | $f$ |
|---|---|---|---|---|---|
| | T (°C) | $T_C$ | $T_E$ | $T_G$ | $T_A$ |
| | | **35** | **90** | **90** | **130** |
| Water | LiBr[1]* | 0.50 | 0.64 | 0.07 | 11.00 |
| TFE | E181[2]* | 0.42 | 0.90 | 0.10 | 9.00 |
| Water | [EMIM][DMP][3]* | 0.48 | Not mentioned | Not mentioned | Not mentioned |
| Water | [DMIM][DMP] | 0.45 | 0.92 | 0.09 | 10.01 |
| Water | [EMIM][DMP] | 0.44 | 0.92 | 0.08 | 11.26 |
| Water | [EMIM][DEP] | 0.44 | 0.92 | 0.07 | 13.54 |
| Water | [EMIM][AC] | 0.44 | 0.87 | 0.08 | 10.54 |
| Water | [HOEtMIM][Cl] | 0.45 | 0.94 | 0.10 | 9.88 |
| Water | [EMIM][$EtSO_4$] | 0.41 | 0.97 | 0.03 | 38.21 |
| Water | [EMIM][Triflate] | 0.42 | 0.99 | 0.02 | 41.34 |
| Water | [EMIM][TFA] | 0.44 | 0.97 | 0.05 | 19.70 |
| Water | [DEMA][Oms] | 0.44 | 0.95 | 0.08 | 12.63 |
| Water | [BMIM][Triflate] | 0.36 | 0.99 | 0.01 | 71.56 |
| Water | [BMIM][$BF_4$] | 0.43 | 0.97 | 0.04 | 25.01 |
| | | **25** | **80** | **80** | **130** |
| Water | LiBr[4]** | 0.48 | Not mentioned | Not mentioned | 9.51 |
| Water | [DMIM][DMP] | 0.43 | 0.93 | 0.06 | 15.92 |
| Water | [EMIM][DMP] | 0.41 | 0.93 | 0.05 | 19.52 |
| Water | [EMIM][DEP] | 0.42 | 0.92 | 0.04 | 21.06 |
| Water | [EMIM][AC] | 0.43 | 0.87 | 0.05 | 17.98 |
| Water | [HOEtMIM][Cl] | 0.43 | 0.95 | 0.06 | 15.58 |
| Water | [EMIM][$EtSO_4$] | 0.14 | 0.97 | 0.01 | 172.47 |
| Water | [EMIM][Triflate] | 0.38 | 0.99 | 0.01 | 69.49 |
| Water | [EMIM][TFA] | 0.42 | 0.97 | 0.03 | 31.99 |
| Water | [DEMA][Oms] | 0.43 | 0.96 | 0.05 | 21.07 |
| Water | [BMIM][Triflate] | 0.27 | 0.99 | 0.01 | 140.50 |
| Water | [BMIM][$BF_4$] | 0.40 | 0.97 | 0.02 | 43.60 |
| | | **20** | **80** | **80** | **130** |
| Water | [DMIM][DMP] | 0.44 | 0.94 | 0.07 | 12.90 |
| Water | [EMIM][DMP] | 0.42 | 0.94 | 0.06 | 15.09 |
| Water | [EMIM][AC] | 0.43 | 0.89 | 0.06 | 14.16 |
| Water | [EMIM][DEP] | 0.43 | 0.88 | 0.93 | 17.71 |
| Water | [HOEtMIM][Cl] | 0.43 | 0.96 | 0.07 | 13.14 |
| Water | [EMIM][$EtSO_4$] | 0.35 | 0.98 | 0.01 | 74.48 |

| Refrigerant | Absorbent | COP | $x^m{}_s$ | $\Delta x^m$ | $f$ |
|---|---|---|---|---|---|
| | T (°C) | $T_C$ | $T_E$ | $T_G$ | $T_A$ |
| Water | [EMIM][Triflate] | 0.39 | 0.99 | 0.02 | 60.08 |
| Water | [EMIM][TFA] | 0.42 | 0.98 | 0.04 | 26.58 |
| Water | [DEMA][Oms] | 0.43 | 0.97 | 0.06 | 17.30 |
| Water | [BMIM][Triflate] | 0.32 | 0.99 | 0.01 | 108.71 |
| Water | [BMIM][$BF_4$] | 0.41 | 0.98 | 0.03 | 34.96 |

* Data found in the literature [8].** Data found in the literature [60].

**Table 3.** Calculated COP of {$H_2O$ + ILs} binary systems for single-effect absorption heat transformer cycle.

In this work, evaporating temperature $T_E$, condensing temperature $T_C$, absorbing temperature $T_A$, and generator temperature $T_G$ are set to 80°C, 20°C, 130°C, and 80°C, respectively (**Figures 6** and **7** and **Table 3**).

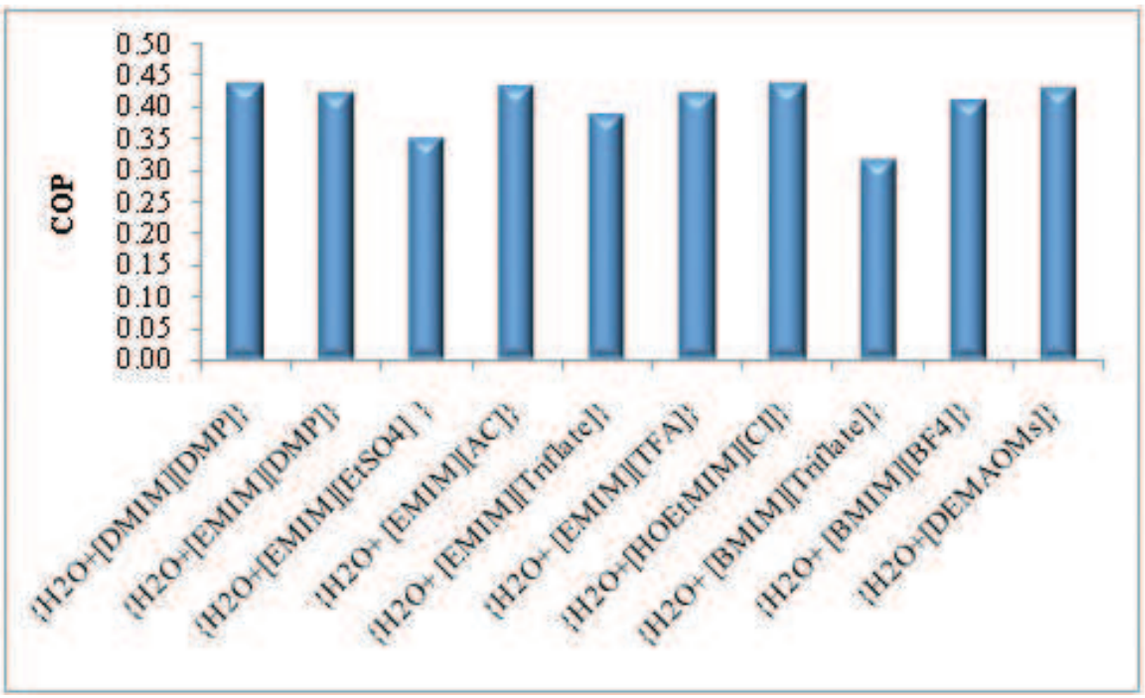


**Figure 6.** Calculated COP of binary systems {water + ILs} presented.

The NRTL model, $C_p$, $H^E$, and density correlation parameters that were regressed by the authors and used for the simulations. The resulting calculated COP values for 12 binary systems are shown in **Table 3**.

The influence of the working temperature levels on the COP is shown in **Figures 8–10**.

http://dx.doi.org/10.5772/65756

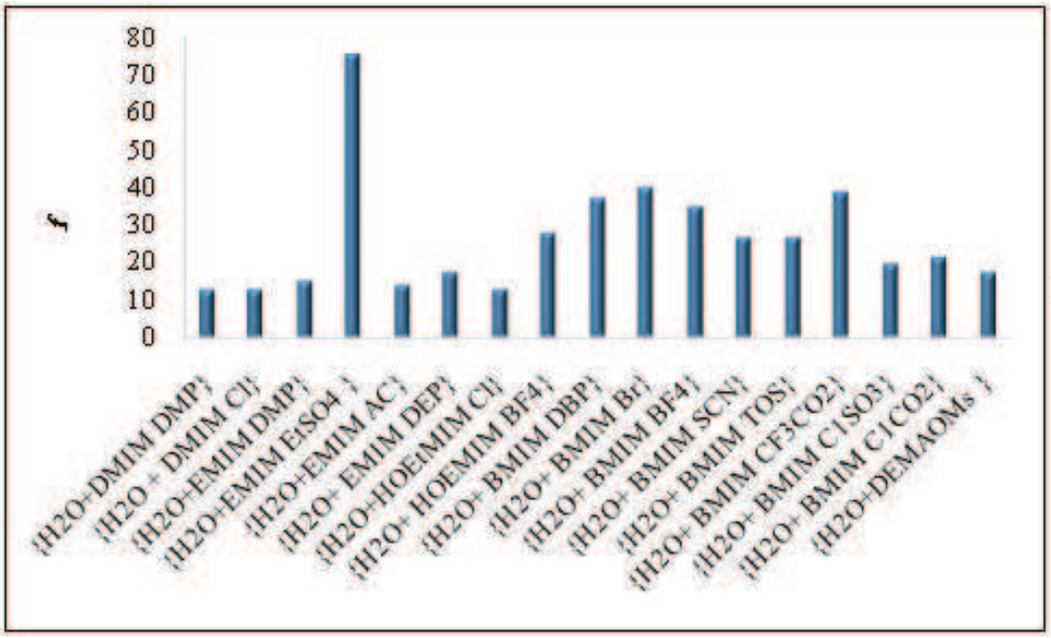


**Figure 7.** Circulation ratio *f* of binary systems {water + ILs} presented.

**Figure 8** shows that an increase in the condenser temperature leads to a decrease in the COP. This behavior is due to the fact that the low pressure level evolves the same way as the condenser temperature. Hence, when the condenser temperature increases, the strong solution ionic liquid fraction will decrease and *f* increases. For the investigated working pairs, the COP remains unchanged for $T_C$ lower than 30°C. The COP sharply decreases especially for {$H_2O$ + LiBr}, {$H_2O$ + [BMIM][$MeSO_4$]}, {$H_2O$ + [BMIM][Triflate]}, and {$H_2O$ + [EMIM][$EtSO_4$]} when $T_C$ is higher than 30°C.

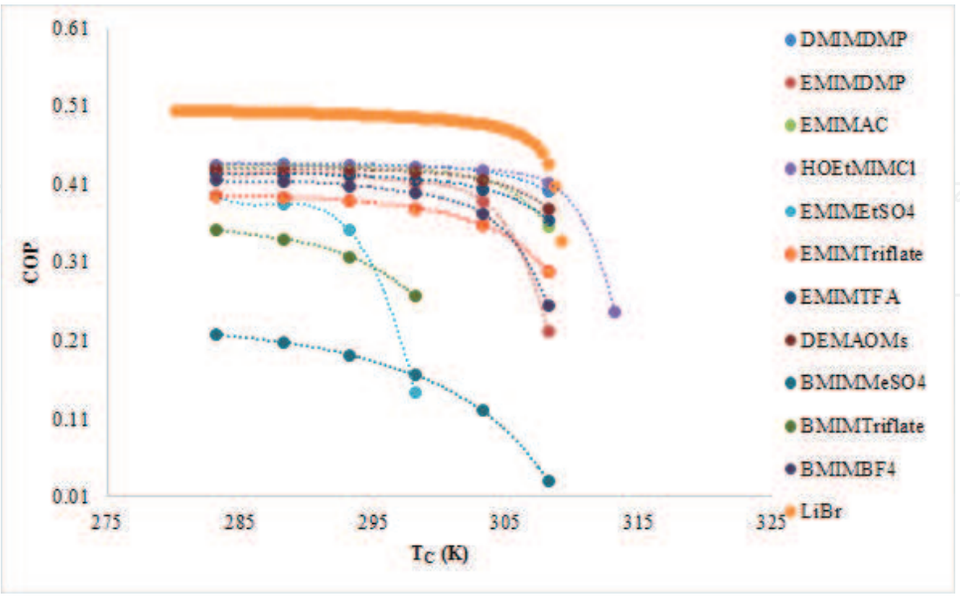


**Figure 8.** COP of binary systems {water + ILs} versus ($T_c$) $T_L$ for single-effect absorption heat transformer cycle.

**Figure 9** shows that an increase of $T_E$ or $T_G$ leads to an increase of the COP. In fact, the high pressure level of AHT depends on the evaporator temperature. Increasing $T_E$ (or $T_G$) leads to a decrease of the weak solution concentration by decreasing the flow ratio. The lower flow ratio results in a higher heat flow released during absorption and consequently in a higher COP. **Figure 9** shows that the evolution of the COP values versus the generator temperature is quite similar to {$H_2O$ + IL} for all binary systems studied in this work. The evolution of COP values with $T_G$ firstly increases, then stabilizes and finally decreases. When $T_G$ approaches its minimal value, $f$ tends to reach infinity and so it requires the generation of heat. Consequently, the COP of the cycle tends toward zero. With the increase of generator temperature, $f$ decreases, COP sharply increases and then smoothens.

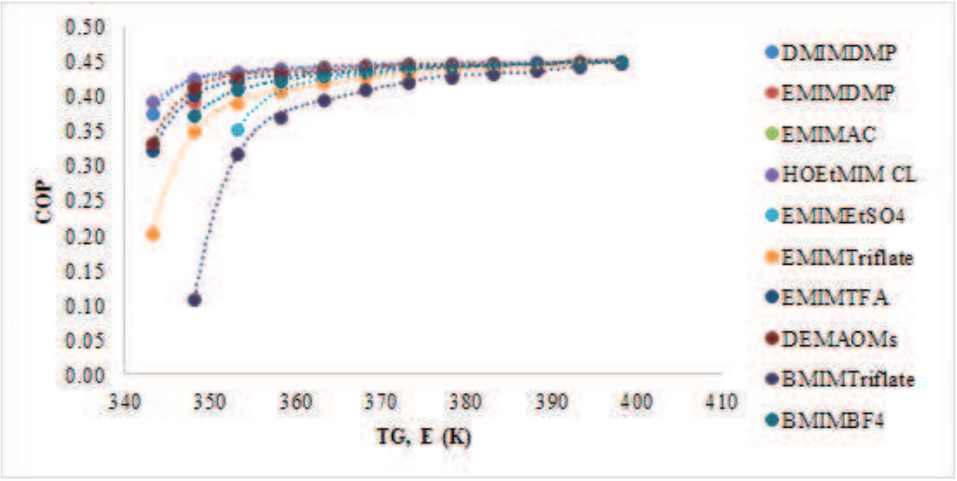


**Figure 9.** COP of binary systems {water + ILs} versus ($T_{G,\ E}$) $T_M$ for single-effect absorption heat transformer cycle.

It can be seen from **Figure 10** that the COP of an AHT decreases at different rates depending on the working mixture when absorber temperature ($T_A$) increases. This behavior can be explained in **Figure 11** that illustrates the ionic liquid mass fraction variation of the weak solution $x^m{}_w$ with $T_A$.

A decrease of $x^m{}_w$ means that the less refrigerant has been absorbed and consequently less heat is released at the absorber, which leads to lower the COP. The same behavior was observed by Zhang and Hu [8]. **Figure 10** shows that the COP of all the binary systems {$H_2O$ + IL} as well as {$H_2O$ + LiBr} is basically unchanged when the gross temperature lift is lower than 45 °C. Upon increasing the gross temperature lift more than 45°C, the COP of {$H_2O$ + LiBr} and {$H_2O$ + ILs} sharply decreases.

The available heat output per unit mass of refrigerant ($q$) for the studied binary systems was calculated and compared with Zhang and Hu [8] data under the same conditions. It was found that $q$ for {$H_2O$ + [DMIM][DMP]} is 2029 kJ $kg^{-1}$ and for {$H_2O$ + [HOEtMIM][Cl]} is less than 2026 kJ $kg^{-1}$. For the other binary systems, $q$ ranges between 2012 and 1527 kJ $kg^{-1}$ (**Table 4**).

These values must be compared with those obtained for {$H_2O$ + LiBr}: 2466 kJ $kg^{-1}$ and 311 kJ $kg^{-1}$ for {TFE + E181}. Hence, to produce the same amount of useful heat, the refrigerant flow rate is lower when using water-based mixtures (water latent heat of vaporization is much higher than that of E181).

http://dx.doi.org/10.5772/65756

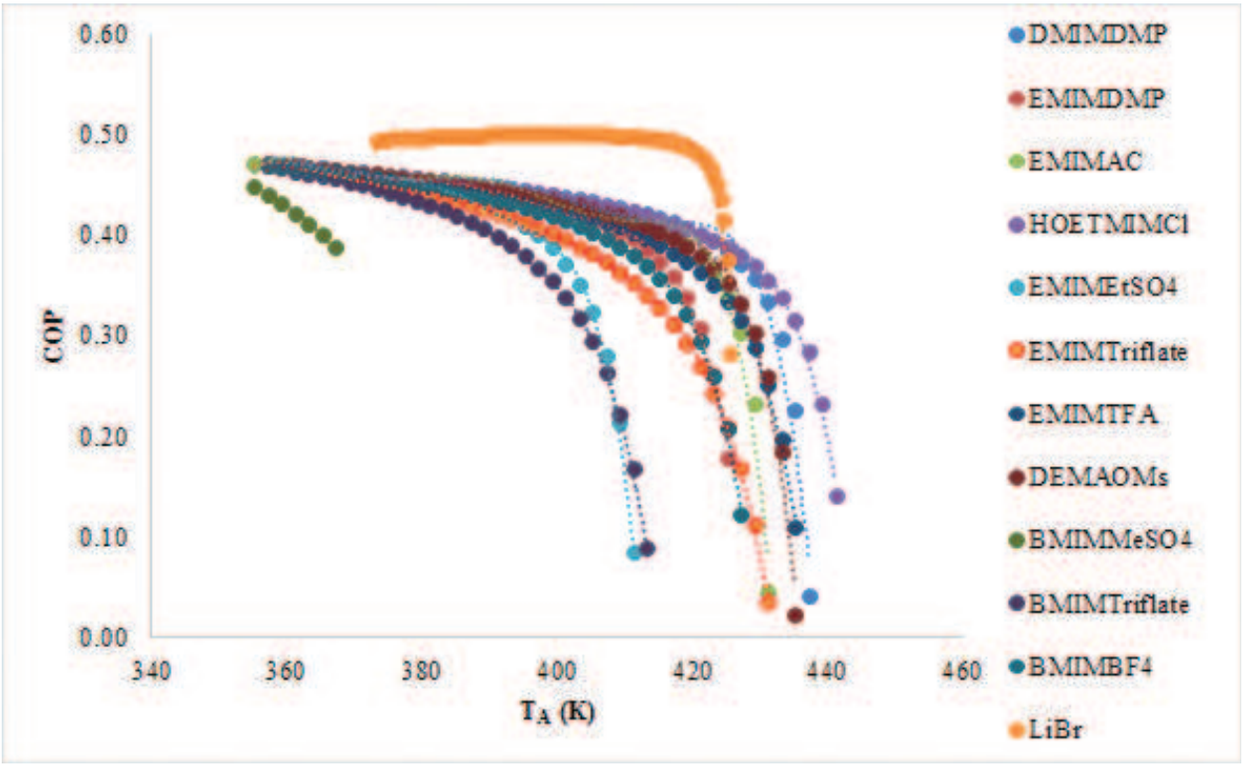


**Figure 10.** COP of binary systems {water + ILs} versus ($T_A$) $T_H$ for single-effect absorption heat transformer cycle.

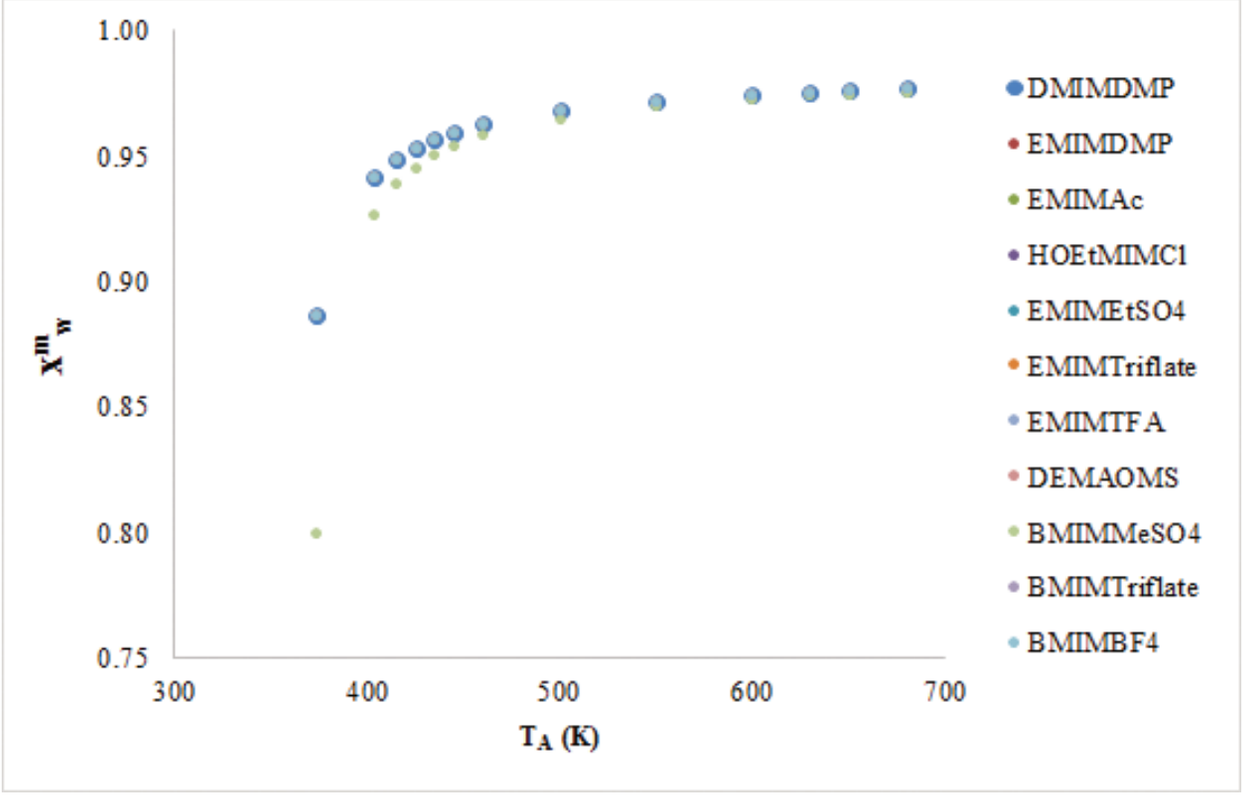


**Figure 11.** Effect of ($T_A$) $T_H$ on $x^m{}_w$.

| $T_C$ | $T_G$ | $T_E$ | $T_A$ |
|---|---|---|---|
| **20** | **80** | **80** | **130** |

| **Binary system** | $q$ **(kJ kg$^{-1}$)** | **Binary system** | $q$ **(kJ kg$^{-1}$)** |
|---|---|---|---|
| {$H_2O$ + [DMIM][DMP]} | 1982.31 | {$H_2O$ + [EMIM][TFA]} | 1871.63 |
| {$H_2O$ + [EMIM][DMP]} | 1867.90 | {$H_2O$ + [HOEtMIM][Cl]} | 1974.05 |
| {$H_2O$ + [EMIM][$EtSO_4$]} | 1391.97 | {$H_2O$ + [BMIM][Triflate]} | 1198.78 |
| {$H_2O$ + [EMIM][AC]} | 1953.77 | {$H_2O$ + [BMIM][$BF_4$]} | 1777.21 |
| {$H_2O$ + [EMIM][Triflate]} | 1636.28 | {$H_2O$ + [DEMA][OMs]} | 1932.00 |

**Table 4.** The available heat output per unit mass of refrigerant ($q$) for AHT cycle.

The concentration (mass fraction) of ILs in the strong solution is exceeding 0.9 for most of the binary systems studied, and is only 0.64 for {$H_2O$ + LiBr} (**Table 3**). This behavior is not in favor of ionic liquid-based working mixtures and will particularly lead to increased pumping costs.

Simulation results show that for {$H_2O$ + [DMIM][DMP]}, {$H_2O$ + [HOEtMIM][Cl]}, {$H_2O$ + [EMIM][Ac]}, {$H_2O$ + [EMIM][TFA]}, and {$H_2O$ + [DEMA][OMS]} mixtures, COP values are close to, but lower than, that obtained working with {$H_2O$ + LiBr}. Nevertheless, these slightly low performances of ionic liquid-based mixtures can be counterbalanced by the ability to reach higher gross temperature lifts and to potentially avoid corrosion issues.

Simulations for evaporator temperature $T_E$, condenser temperature $T_C$, absorber temperature $T_A$, and generator temperature $T_G$ are set to 80, 20, 130, and 80 °C, respectively, which shows that the COP values for the studied binary systems have the following behavior:

[DMIM][DMP] > [HOEtMIM][Cl] > [EMIM][Ac] > [DEMA][OMS] > [EMIM][TFA] > [EMIM][DMP] > [BMIM][$BF_4$] > [EMIM][Triflate] > [EMIM][$EtSO_4$] > [BMIM][Triflate]. We can conclude that ionic liquids with a short-alkyl chain lead to higher COP values and a lower circulation ratio $f$.

Simulations indicate that binary systems {$H_2O$ + acetate or chloride-based ILs} have high COP. Nonetheless, these families of ILs are not sufficiently stable and they present high corrosion rates [50]. It was noticed that binary system composed of {$H_2O$ + [BMIM][$MeSO_4$]} exhibits smaller $\Delta t$ than the other investigated 11 systems. Its largest observed $\Delta t$ is about 40 K and the lowest is 30 K. Simulation of the binary system consisting of {$H_2O$ + [BMIM][$MeSO_4$]} is not promising due to low solubility of IL in water or to stability of the IL [16].

Thirty-three binary systems out of 39 are found to have only VLE data available, the literature lacking other thermodynamic properties. Using NRTL, the VLE data of these 33 binary systems were correlated, and $f$ was determined. Simulations for these binary systems performed with evaporator temperature $T_E$, condenser temperature $T_C$, absorber temperature $T_A$, and generator temperature $T_G$ are set to 80°C, 20°C, 130°C, and 80°C, respectively. Simulation results showed that there are promising binary systems exhibiting low $f$ values such as [BMIM][$C_1SO_3$], [BMIM][I], [BMPyr][DCA], which are 19.892, 16.958, and 17.247, respectively.

In the light of these results, it would be highly recommended to further investigate these binary systems.

## 6. Conclusion

A large number of binary mixtures {$H_2O$ + ILs} have been identified to be used in absorption heat transformers. The resulting performances of these new working fluids were evaluated for single-effect absorption heat transformer cycles.

Ionic liquid-based working mixtures lead to slightly low COP than the classical {$H_2O$ + LiBr} mixture and larger circulation ratios. Nevertheless, the possibility to find ILs that are significantly less corrosive than LiBr is a condition for reliable operation and a moderate investment cost. Moreover, many ILs are totally miscible with water which avoid crystallization problems.

It must be kept in mind that thermal and chemical stability of {$H_20$ + IL} mixtures have to be assessed in order to prove their practical use for industrial applications.

## Author details

El-Shaimaa Abumandour, Fabrice Mutelet* and Dominique Alonso

*Address all correspondence to: fabrice.mutelet@univ-lorraine.fr

Laboratoire Réactions et Génie des Procédés (CNRS UMR 7274), Ecole Nationale Supérieure des Industries Chimiques, Université de Lorraine, Nancy, France

## References

[1] Horuz I, Kurt B. Absorption heat transformers and an industrial application. Renewable Energy. 2010;**35**:2175–81. DOI: 10.1016/j.renene.2010.02.025

[2] Khamooshi M, Parham K, Atikol U. Overview of ionic liquids used as working fluids in absorption cycles. Advances in Mechanical Engineering. 2013;**2013**:1–7. DOI: org/10.1155/2013/620592

[3] Sun J, Fu L, Zhang S. A review of working fluids of absorption cycles. Renewable and Sustainable Energy Reviews. 2012;**16**:1899–1906. DOI: 10.1016/j.rser.2012.01.011

[4] Schaefer LA. Single pressure absorption heat pump analysis [thesis]. Georgia: Georgia Institute of Technology; 2000.

[5] Wu W, Wang B, Shi W, Li X. An overview of ammonia-based absorption chillers and heat pumps. Renewable and Sustainable Energy Reviews. 2014;**31**:681−707. DOI: org/10.1016/j.rser.2013.12.021

[6] Srikhirin P, Aphornratana S, Chungpaibulpatana S. A review of absorption refrigeration technologies. Renewable and Sustainable Energy Reviews. 2001;**5**:343–372. DOI: 10.1016/S1364-0321(01)00003-X

[7] Dong L, Zheng D, Nie N, Li Y. Performance prediction of absorption refrigeration cycle based on the measurements of vapor pressure and heat capacity of {H2O + [DMIM][DMP]} system. Applied Energy. 2012;**98**:326–332. DOI: org/10.1016/j.apenergy.2012.03.044

[8] Zhang X, Hu D. Performance analysis of the single-stage absorption heat transformer using a new working pair composed of ionic liquid and water. Applied Thermal Engineering. 2012;**37**:129–135. DOI: 10.1016/j.applthermaleng.2011.11.006

[9] De Lucas A, Donate M, Molero C, Villasenor J, Rodríguez JF. Performance evaluation and simulation of a new absorbent for an absorption refrigeration system. International Journal of Refrigeration. 2004;**27**:324–330. DOI: 10.1016/j.ijrefrig.2003.12.008

[10] Kurnia KA, Coutinho Joao AP. Overview of the excess enthalpies of the binary mixtures composed of molecular solvents and ionic liquids and their modeling using COSMO-RS. Industrial & Engineering Chemistry Research2013;**52**:13862–13874. DOI: 10.1021/ie4017682

[11] Kim S, Patel N, Kohl PA. Performance simulation of ionic liquid and hydrofluorocarbon working fluids for an absorption refrigeration system. Industrial & Engineering Chemistry Research 2013;**52**:6329–6335. DOI: 10.1021/ie400261g

[12] Kim S, Kim YJ, Joshi YK, Fedorov AG, Kohl PA. Absorption heat pump/refrigeration system utilizing ionic liquid and hydrofluorocarbon refrigerants. Journal of Electronic Packaging. 2012;**134**:031009–9. DOI: 10.1115/1.4007111

[13] Zheng D, Dong L, Huang W, Wu X, Nie N. A review of imidazolium ionic liquids research and development towards working pair of absorption cycle. Renewable and Sustainable Energy Reviews. 2014;**37**:47–68. DOI: 10.1016/j.rser.2014.04.046

[14] Iolitec. Product, N. Ionic Liquids Today. 2011;**1**:1–11.

[15] Liang S, Chen W, Cheng K, Guo Y, Gui X. The Latent Application of Ionic Liquids in Absorption Refrigeration. In: Prof. Scott Handy, editors. Applications of Ionic Liquids in Science and Technology, Croatia. InTech; 2011. 494 p. DOI: 10.5772/23953

[16] Ficke LE. Thermodynamic properties of imidazolium and phosphonium based ionic liquid mixtures with water or carbon dioxide [thesis]. Notre Dame: Graduate School of the University of Notre Dame; 2010.

[17] Nakanishi T, Furukawa T, Sato N. Industrial high-temperature heat pump. Hitachi Zosen Technical Review . 1981;**42**:7–12.

[18] Kim S, Kohl PA. Analysis of [hmim][PF6] and [hmim][Tf2N] ionic liquids as absorbents for an absorption refrigeration system. International Journal of Refrigeration. 2014;**48**:105–113. DOI: 10.1016/j.ijrefrig.2014.09.003

[19] Merkel N, Weber C, Faust M, Schaber K. Influence of anion and cation on the vapor pressure of binary mixtures of water plus ionic liquid and on the thermal stability of the ionic liquid. Fluid Phase Equilibria. 2015;**394**:29–37. DOI: org/10.1016/j.fluid.2015.03.00

[20] Wu W, Wang B, Shi W, Li X. Absorption heating technologies: A review and perspective. Applied Energy. 2014;**130**:51–71. DOI: org/10.1016/j.apenergy.2014.05.027

[21] Grossman G. Absorption heat transformer for process heat generation from solar ponds. ASHRAE Transactions. 1991;**97**:420–427.

[22] Ikeuchi M, Yumikura T, Ozaki E, Yamanaka G. Design and performance of a high-temperature- boost absorption heat pump. ASHRAE Transactions. 1985;**91**:2081–94.

[23] Zawadzki M, Krolikowska M, Lipinski P. Physicochemical and thermodynamic characterization of N-alkyl-N-methylpyrrolidinium bromides and its aqueous solutions. Thermochimica Acta. 2014;**589**:148–157. DOI: 10.1016/j.tca.2014.05.028

[24] Merkel NC, Romich C, Bernewitz R, Kunemund H, Gleiß M, Sauer S, Schubert TJS, Guthausen G, Schaber K. Thermophysical properties of the binary mixture of water + diethylmethylammonium trifluoromethanesulfonate and the ternary mixture of water + diethylmethylammonium trifluoromethanesulfonate + diethylmethylammonium methanesulfonate. Journal of Chemical & Engineering Data. 2014;**59**:560−570. DOI: org/10.1021/je400097

[25] Ren J, Zhao Z, Zhang X. Vapor pressures, excess enthalpies, and specific heat capacities of the binary working pairs containing the ionic liquid 1-ethyl-3-methylimidazolium dimethylphosphate. Journal of Chemical Thermodynamics. 2011;**43**:576–583. DOI: 10.1016/j.jct.2010.11.014

[26] Gong Y, Shen C, Lu Y, Meng H, Li CX. Viscosity and density measurements for six binary mixtures of water (methanol or ethanol) with an ionic liquid ([BMIM][DMP] or [EMIM][DMP]) at atmospheric pressure in the temperature range of (293.15 to 333.15). Journal of Chemical & Engineering Data. 2012;**57**: 33–39. DOI: org/10.1021/je200600

[27] Zhang X, Hu D. Performance simulation of the absorption chiller using water and ionic liquid 1-ethyl-3-methylimidazolium dimethylphosphate as the working pair. Applied Thermal Engineering. 2011;**31**:3316–21. DOI: 10.1016/j.applthermaleng.2011.06.011

[28] Kato R, Gmehling J. Measurement and correlation of vapor–liquid equilibria of binary systems containing the ionic liquids [EMIM][(CF3SO2)2N], [BMIM][(CF3SO2)2N], [MMIM][(CH3)2PO4] and oxygenated organic compounds respectively water. Fluid Phase Equilibria. 2005;**231**:38–43. DOI: 10.1016/j.fluid.2005.01.00

[29] Wang J, Wang D, Li Z, Zhang F. Vapor pressure measurement and correlation or prediction for water, 1-propanol, 2-propanol, and their binary mixtures with [MMIM][DMP] ionic liquid. Journal of Chemical & Engineering Data. 2010;**55**:4872–4877. DOI: 10.1021/je100483d

[30] Wang JF, Li CX, Wang ZH, Li ZJ, Jiang YB. Vapor pressure measurement for water, methanol, ethanol, and their binary mixtures in the presence of an ionic liquid1-ethyl-3-methylimidazolium dimethylphosphate. Fluid Phase Equilibria. 2007;**255**:186–192. DOI: 10.1016/j.fluid.2007.04.010

[31] Yokozeki A, Shiflett MB. Water solubility in ionic liquids and application to absorption cycles. Industrial & Engineering Chemistry Research. 2010;**49**:9496–9503. DOI: 10.1021/ie1011432

[32] Zuo G, Zhao Z, Yan S, Zhang X. Thermodynamic properties of a new working pair: 1-ethyl-3-methylimidazolium ethylsulfate and water. Chemical Engineering Journal. 2010;**156**:613−617. DOI: 10.1016/j.cej.2009.06.020

[33] Romich C, Merkel NC, Valbonesi A, Schaber K, Sauer S, Schubert TJS. Thermodynamic properties of binary mixtures of water and room temperature ionic liquids: vapor pressure, heat capacities, densities and viscosities of water + 1-ethyl-3-methylimidazolium acetate and water + diethylmethylammonium methane sulfonate. Journal of Chemical & Engineering Data. 2012;**57**:2258−2264. DOI: org/10.1021/je300132

[34] Fendt S, Padmanabhan S, Blanch HW, Prausnitz JM. Viscosities of acetate or chloride-based ionic liquids and some of their mixtures with water or other common solvents. Journal of Chemical & Engineering Data. 2011;**56**:31–34. DOI: 10.1021/je1007235

[35] Nie N, Zheng D, Dong L, Li Y. Thermodynamic properties of the water + 1- (2-hydroxylethyl)-3-methylimidazolium chloride system. Journal of Chemical & Engineering Data. 2012;**57**:3598−3603. DOI: org/10.1021/je3007953

[36] He Z, Zhao Z, Zhang X, Feng H. Thermodynamic properties of new heat pump working pairs: 1, 3-dimethylimidazolium dimethylphosphate and water, ethanol and methanol. Fluid Phase Equilibria. 2010; **298**:83–91. DOI: 10.1016/j.fluid.2010.07.00

[37] Zhao J, Jiang XC, Li CX, Wang ZH. Vapor pressure measurement for binary and ternary systems containing a phosphoric ionic liquid. Fluid Phase Equilibria. 2006;**247**:190–198. DOI: 10.1016/j.fluid.2006.07.00

[38] Alevizou EI, Pappa GD, Voutsas EC. Prediction of phase equilibrium in mixtures containing ionic liquids using UNIFAC. Fluid Phase Equilibria. 2009;**284**:99–105. DOI: 10.1016/j.fluid.2009.06.01

[39] Passos H, Khan I, Mutelet F, Oliveira MB, Carvalho PJ, Santos LMN BF, Held C, Sadowski G, Freire MG, Coutinho JAP. Vapor-liquid equilibria of water + alkylimidazolium-based ionic liquids: measurements and perturbed-chain statistical associating fluid theory modeling. Industrial & Engineering Chemistry Research. 2014;**53**:3737–48. DOI: org/10.1021/ie4041093

[40] Llovell F, Valente E, Vilaseca O, Vega LF. Modeling complex associating mixtures with [Cn-mim][Tf2N] ionic liquids: predictions from the Soft-SAFT equation. Journal of Physical Chemistry B. 2011;**115**:4387–4398. DOI: org/10.1021/jp112315b

[41] Chen Y, Mutelet F, Jaubert JN. Experimental measurement and modeling of phase diagrams of binary systems encountered in the gasoline desulfurization process using ionic liquids. Journal of Chemical & Engineering Data. 2014;**59**:603–612. DOI: org/10.1021/je400510

[42] Nann A, Held C, Sadowski G. Liquid-liquid equilibria of 1-butanol/water/IL systems. Industrial & Engineering Chemistry Research. 2013;**52**:18472–18481. DOI: org/10.1021/ie403246

[43] Shariati A, Peters CJ. High-pressure phase behavior of systems with ionic liquids: measurements and modeling of the binary system fluoroform+1-ethyl-3-methylimidazolium hexafluorophosphate. Journal of Supercritical Fluids. 2003;**25**:109–117. DOI: 10.1016/S0896-8446(02)00160-2

[44] Carvalho PJ, Alvarez VH, Machado JJB, Pauly J, Daridon JL, Marrucho IM, Aznar M, Coutinho JAP. High pressure phase behavior of carbon dioxide in 1-alkyl-3-methylimidazolium bis(trifluoromethylsulfonyl) imide ionic liquids. Journal of Supercritical Fluids. 2009;**48**:99–107. DOI: 10.1016/j.supflu.2008.10.01

[45] Ren W, Scurto AM. Phase equilibria of imidazolium ionic liquids and the refrigerant gas, 1, 1, 1, 2-tetrafluoroethane (R-134a). Fluid Phase Equilibria. 2009;**286**:1–7. DOI: 10.1016/j.fluid.2009.07.007

[46] Seddon KR, Stark A, Torres MJ. Influence of chloride, water, and organic solvents on the physical properties of ionic liquids. Pure and Applied Chemistry. 2000;**72**:2275–87. DOI: 10.1351/pac200072122275

[47] Morrissey AJ, O'Donnell JP. Endothermic solutions and their application in absorption heat pumps. Chemical Engineering Research and Design. 1986;**64**:404−406.

[48] Lungwitz R, Spange S. A hydrogen bond accepting (HBA) scale for anions, including room temperature ionic liquids. New Journal of Chemistry. 2008;**32**:392−394. DOI: 10.1039/b714629a

[49] Cao YY, Chen Y, Lu L, Xue ZM, Mu TC. Water sorption in functionalized ionic liquids: kinetics and intermolecular interactions. Industrial & Engineering Chemistry Research 2013;**52**:2073−83. DOI: org/10.1021/ie302850z

[50] Seiler M, Kühn A, Ziegler F, Wang X. Sustainable cooling strategies using new chemical system solutions. Industrial & Engineering Chemistry Research. 2013;**52**:16519−16546. DOI: org/10.1021/ie401297u

[51] Hu HC, Soriano AN, Leron RB, Li MH. Molar heat capacity of four aqueous ionic liquid mixtures. Thermochimica Acta. 2011;**519**:44–49. DOI: 10.1016/j.tca.2011.02.027

[52] Lashkarbolooki M, Hezave AZ, Ayatollahi S. Artificial neural network as an applicable tool to predict the binary heat capacity of mixtures containing ionic liquids. Fluid Phase Equilibria. 2012;**324**:102–107. DOI: 10.1016/j.fluid.2012.03.015

[53] Carvalho PJ, Alvarez VH, Marrucho IM, Aznar M, Coutinho JAP. High carbon dioxide solubilities in trihexyl tetradecylphosphonium-based ionic liquids. Journal of Supercritical Fluids. 2010;**52**:258–265. DOI: 10.1016/j.supflu.2010.02.00

[54] Carvalho PJ, Alvarez VH, Marrucho IM, Aznar M, Coutinho JAP. High pressure phase behavior of carbon dioxide in 1-butyl-3-methylimidazolium bis (trifluoromethylsulfonyl) imide and 1-butyl-3-methylimidazolium dicyanamide ionic liquids. Journal of Supercritical Fluids. 2009;**50**:105–111. DOI: 10.1016/j.supflu.2009.05.00

[55] Ficke LE, Rodriguez H, Brennecke JF. Heat capacities and excess enthalpies of 1-ethyl-3-methylimidazolium-based ionic liquids and water. Journal of Chemical & Engineering Data. 2008;**53**:2112–2119. DOI: 10.1021/je800248w

[56] Garcia-Miaja G, Troncoso J, Romani L. Excess enthalpy, density, and heat capacity for binary systems of alkylimidazolium-based ionic liquids + water. Journal of Chemical Thermodynamics. 2009;**41**:161−166. DOI: 10.1016/j.jct.2008.10.002

[57] Dong L, Zheng DX, Wei Z, Wu XH. Synthesis of 1,3-dimethylimidazolium chloride and volumetric property investigations of its aqueous solution. International Journal of Thermophysics. 2009;**30**:1480–1490. DOI: 10.1007/s10765-009-0651-x

[58] Lehmann J, Rausch MH, Leipertz A, Froba AP. Densities and excess molar volumes for binary mixtures of ionic liquid 1-ethyl-3-methylimidazolium ethylsulfate with solvents. Journal of Chemical & Engineering Data. 2010;**55**:4068−4074. DOI: 10.1021/je1002237

[59] Vercher E, Orchilles AV, Miguel PJ, Martinez-Andreu A. Volumetric and ultrasonic studies of 1-ethyl-3-methylimidazolium trifluoromethanesulfonate ionic liquid with methanol, ethanol, 1-propanol, and water at several temperatures. Journal of Chemical & Engineering Data. 2007;**52**:1468−1482. DOI: 10.1021/je7001804

[60] Chakrabarty D, Chakraborty A, Seth D, Sarkar N. Effect of water, methanol, and acetonitrile on solvent relaxation and rotational relaxation of coumarin 153 in neat 1-hexyl-3-methylimidazolium hexafluorophosphate. Journal of Physical Chemistry A. 2005;**109**:1764–1769. DOI: 10.1021/jp0460339

[61] Gonzalez EJ, Dominguez A, Macedo EA. Physical and excess properties of eight binary mixtures containing water and ionic liquids. Journal of Chemical & Engineering Data. 2012;**57**:2165−2176. DOI: org/10.1021/je201334p

[62] Bahadur I, Letcher TM, Singh S, Redhi GG, Venkatesu P, Ramjugernath D. Excess molar volumes of binary mixtures (an ionic liquid + water): A review. Journal of Chemical Thermodynamics. 2015;**82**:34–46. DOI: org/10.1016/j.jct.2014.10.003

[63] Kim YJ, Kim S, Joshi YK, Fedorov AG, Kohl PA. Thermodynamic analysis of an absorption refrigeration system with ionic-liquid/refrigerant mixture as a working fluid. Energy. 2012;**44**:1005–1016. DOI: 10.1016/j.energy.2012.04.048

[64] Rodriguez H, Brennecke JF. Temperature and composition dependence of the density and viscosity of binary mixtures of water + ionic liquid. Journal of Chemical & Engineering Data. 2006;**51**:2145−2155. DOI: 10.1021/je0602824

[65] Pandey S, Fletcher KA, Baker SN, Baker GA. Correlation between the fluorescent response of microfluidity probes and the water content and viscosity of ionic liquid and water mixtures. Analyst. 2004;**129**:569–573. DOI: 10.1039/B402145M

[66] Rebelo LPN, Najdanovic-Visak V, Visak ZP, Da Ponte MN, Szydlowski J, Cerdeirina CA, Troncoso J, Romani L, Esperanca JMSS, Guedes HJR, De Sousa HC. A detailed thermodynamic analysis of [C4mim][BF4] + water as a case study to model ionic liquid aqueous solutions. Green Chemistry. 2004;**6**:369–381. DOI: 10.1039/B400374H

[67] Ayou DS, Curras MR, Salavera D, Garcia J, Bruno JC, Coronas A. Performance analysis of absorption heat transformer cycles using ionic liquids based on imidazolium cation as absorbents with 2, 2, 2-trifluoroethanol as refrigerant. Energy Conversion and Management. 2014;**84**:512–523. DOI: 10.1016/j.enconman.2014.04.077

[68] Wooster TJ, Johanson KM, Fraser KJ, MacFarlane DR, Scott JL. Thermal degradation of cyano containing ionic liquids. Green Chemistry. 2006;**8**:691−696. DOI: 10.1039/B606395K

[69] Ngo HL, LeCompte K, Hargens L, McEwen AB. Ngo HL, LeCompte K, Hargens L, McEwen AB. Thermal properties of imidazolium ionic liquids. Thermochimica Acta. 2000;**357–358**:97−102. DOI: 10.1016/S0040-6031(00)00373-7

[70] Baranyai KJ, Deacon GB, Mac FDR, Pringle JM, Scott JL. Thermal degradation of ionic liquids at elevated temperatures. Australian Journal of Chemistry. 2004;**57**:145−147. DOI: 10.1071/CH03221

[71] Huangfu L, Wu X, Guo K, Ding N. Heat characteristics research of a water-soluble ionic liquid as absorption workers. Chinese Journal of Analytical Chemistry. 2011;**50**:39−44.

[72] Freire MG, Neves CMSS, Marrucho IM, Coutinho JAP, Fernandes A M. Hydrolysis of tetrafluoroborate and hexafluorophosphate counter ions in imidazolium-based ionic liquids. Journal of Physical Chemistry A. 2010;**114**:3744–3749. DOI: 10.1021/jp903292n

[73] Islam MM, Ohsako T. Roles of ion pairing on electroreduction of dioxygen in imidazolium-cation-based room-temperature ionic liquid. Journal of Physical Chemistry C. 2008;**112**:1269−1275. DOI: 10.1021/jp7096185

[74] Swatloski RP, Holbrey JD, Memon SB, Caldwell GA, Caldwell KA, Rogers RD. Swatloski RP, Holbrey JD, Memon SB, Caldwell GA, Caldwell KA, Rogers RD. Using Caenorhabditis elegans to probe toxicity of 1-alkyl-3-methylimidazolium chloride based ionic liquids. Chemical Communication. 2004;**6**:668−669. DOI: 10.1039/B316491H

[75] Uerdingen M, Treber C, Balser M, Schmitt G, Werner Ch. Corrosion behavior of ionic liquids. Green Chemistry. 2005;**7**:321–325. DOI: 10.1039/B419320M

[76] Parham K, Khamooshi M, Tematio DBK, Yari M, Atikol U. Absorption heat transformers–A comprehensive review. Renewable and Sustainable Energy Reviews. 2014;**34**:430–452. DOI: org/10.1016/j.rser.2014.03.036

IntechOpen